

Cite this: *Lab Chip*, 2011, **11**, 3816

www.rsc.org/loc

PAPER

Accumulating microparticles and direct-writing micropatterns using a continuous-wave laser-induced vapor bubble†

Yajian Zheng, Hui Liu,* Yi Wang, Cong Zhu, Shuming Wang, Jingxiao Cao and Shining Zhu

Received 1st June 2011, Accepted 25th August 2011

DOI: 10.1039/c1lc20478e

Through the enhanced photothermal effect, which was achieved using a silver film, a low power weakly focused continuous-wave laser (532 nm) was applied to create a vapor bubble. A convective flow was formed around the bubble. Microparticles dispersed in water were carried by the convective flow to the vapor bubble and accumulated on the silver film. By moving the laser spot, we easily manipulated the location of the bubble, allowing us to direct-write micropatterns on the silver film with accumulated particles. The reported simple controllable accumulation method can be applied to bimolecular detection, medical diagnosis, and other related biochip techniques.

Introduction

The techniques for concentration and patterning of micro- or nano-particles have received significant attention for the development of artificial architectures, including accumulation of analytes for enhanced sample detection and diagnosis or colloidal crystals.¹ Over the last few decades, optical traps (optical tweezers) and related techniques have been used increasingly as tools for concentrating and patterning in biology and other fields.^{2–7} However, for conventional optical tweezers, high laser power is required for trapping analytes, although this can bring possible damage to the trapped analytes. Furthermore, the tweezing zone is limited to the small region illuminated by the operating laser. Once the particles adhere to the surface of the substrate through the van der Waals force, it is difficult for conventional optical tweezers to manipulate them.

An improved technology developed in recent years is near-field optical trapping by various nanostructures.^{8–15} Due to the spatially localized electric field and the enhancement of the local energy around these nanostructures, near-field optical trapping can be utilized as a useful tool for concentrating and patterning of microsized/nanosized particles in very small regions. Another accumulation technique is optically induced simultaneous thermophoresis and convection,^{16–21} which has been used to

concentrate DNA¹⁸ and direct assemble nanoparticles.¹⁹ Strong drag force and long-range capturing are two main advantages of this technology. Furthermore, by adjusting the location of the heat source, it is possible to dynamically control the accumulation location of microparticles.

In the present study, we propose a simple method to accumulate microparticles on a silver film with a vapor bubble induced by a low power continuous-wave (CW) laser. Due to the efficient absorption of the laser power, the silver film is quickly heated up, creating a vapor bubble at the laser spot. Then, a thermal convective flow forms around the vapor bubble. Particles in the water are long-range captured by the convective flow, carried to the bubble, and then deposited on the surface of the silver film. By moving the laser spot, we can dynamically control the position of the bubble and the accumulated particles. Thus, we can easily direct write any micropatterns with the accumulated particles on the silver film.

Experimental setup

The experimental setup is illustrated in Fig. 1. It consists of three parts: liquid chambers, Zeiss microscope system, and laser system. A 120 μm thick water sheet was sandwiched between a glass coverslip and SiO_2 substrate covered by a sputtered silver film. Red fluorescent polystyrene particles with 1 μm diameter (Duke Scientific, CA, USA) were dispersed in deionized water. A green laser beam (operating at 532 nm) was expanded, collimated, and focused (beam waist being 106 μm) onto the surface of the silver film. Here, the focusing spot can be moved manually over a short range in the x - y plane. A white light source of an Hg arc lamp (100 W, Zeiss) was used to visualize the bubble and fluorescence particles. Their images were then projected to a CCD camera by a microscope objective (Zeiss Epiplan 5 \times /0.13 HD Microscope Objective).

National Laboratory of Solid State Microstructures & Department of Physics, Nanjing University, Nanjing 210093, People's Republic of China. E-mail: liuhui@nju.edu.cn; Web: <http://dssl.nju.edu.cn/mpp>; Fax: +86-025-83595535; Tel: +86-025-83593091

† Electronic supplementary information (ESI) available: Movie S1 records a vapor bubble being created at the interface between water and silver film; Movie S2 shows the particles being dragged by the convective flow to the bubble; Movie S3 shows the vapor bubble being dragged by the laser spot; Movie S4 illustrates the process of the directly write micropattern with the accumulated particles on the silver film by the vapor bubble. See DOI: 10.1039/c1lc20478e

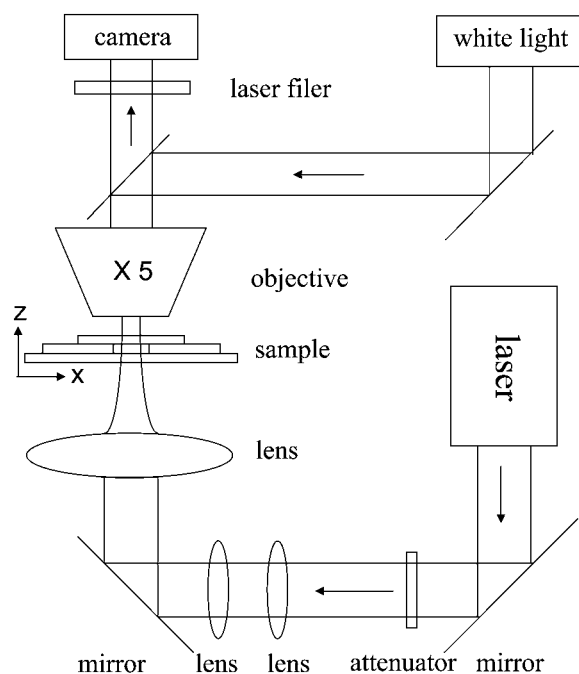


Fig. 1 Schematic representation of the experimental setup. The power of the laser (operating at 532 nm) is regulated using an attenuator. After passing through a telescope, the beam is weakly focused onto the sample with a lens. The focusing spot can be moved manually over a shorter range in the x - y plane. The ordinary image is formed by an Hg arc lamp which illuminates the sample. The transmitted/reflected light is collected by the Zeiss objective and imaged onto a camera *via* a color filter.

Vapor bubble generation

In our experiments, when a 250 mW laser beam was focused on the interface between the silver film and water, the silver film quickly heated up due to the efficient absorption of the laser power. The temperature of water can be raised by the silver film above the boiling point in a very short time. Once the superheat limit of the liquid was reached, a violent phase explosion occurred, and a vapor bubble was created at the interface between water and silver film (see ESI†, Movie S1). The focusing laser spot behaved like a heat point-source to expand and manipulate the bubble. The bubble remained in contact with the substrate throughout the process and displayed a truncated sphere shape after it expanded to reach the cover glass. Recently we were happy to read a latest paper (ref. 22), which reports that the vapor bubble can indeed be created effectively through this method.

Thermal-induced convective flow and accumulation of microparticles

Generally, while creating a vapor bubble, heat from strong absorption of the laser power by the silver film induces a temperature gradient in the liquid simultaneously. This temperature gradient then drives a local convective flow around the bubble. The direction of convection flow is presented in Fig. 2(d). The movement of particles in the convection flow can be described using a simple 1D model: the flux of moving particles is described by $\vec{j} = v(r)c - D\nabla c - D_T c \nabla T$,²⁰ where $v(r)$ is the flow velocity, c is

the concentration, ∇c and ∇T are concentration and temperature gradients, D is the diffusion coefficient, and D_T is the thermal diffusion coefficient. The interpretation of each term in this 1D model is very straightforward: the first term corresponds to the convective drag effect, and the last two terms correspond to free diffusion and thermophoretic process, respectively. When we input a lower power laser (about 100 mW), neither convection nor bubble is created, and we observed the slow motion of the particle ($1\text{--}2 \mu\text{m s}^{-1}$) induced by the thermophoretic effect from the laser spot to the cold region. For this case, as no convection flow is formed, $v(r) = 0$, we could have $\vec{j} = -D\nabla c - D_T c \nabla T$, which means that only diffusion and thermophoretic effects contribute to the motion. However, after the bubble is created and convection is formed $v(r) \neq 0$, the motion of particles will be determined by three forces simultaneously. In this process, the direction of motion induced by convection is contrary to the motion by the diffusion and thermophoretic effect. As the force by convection flow is much larger than other two forces, the motion of particles is dominated by the convection process. Therefore, particles will be carried by the convection flow to the bubble (see Fig. 2(d)). In our experiments, we did observe that the particles moved to the bubble and accumulated around it (see Fig. 2(a–c) and Movie S2 in the ESI†). Furthermore, the observation shows that the moving speed by convection is much faster (about $25 \mu\text{m s}^{-1}$) than the motion by diffusion and thermophoretic effects (about $1\text{--}2 \mu\text{m s}^{-1}$).

Due to the strong upward convection flow along the surface of the bubble, the flow was pushed away from the bubble at the ceiling (cover glass slip) and squeezed to the bubble at the floor (silver film). As a result, the fluorescent particles were dragged by the flow to the bubble. At the corner between the bubble and silver film (see Fig. 2(d)), being very close to the silver film, they are attracted to the silver film by the short-range van der Waals force. In the experiment, for a particle with the diameter of $1.0 \mu\text{m}$ immersed in water, we estimated that the gravity is about 12 fN, the buoyancy is about 5.2 fN, and the convection force is about 0.24 pN when the convection velocity is $25 \mu\text{m s}^{-1}$. All the three forces are long-range forces which are dominant when the distance between the particle and film is large. However, when the distance between the particle and film is below 10 nm, the van der Waals force is above 6 pN which is much larger than the above three forces. Then the van der Waals force is dominant at the corner between the bubble and Ag film (see Fig. 2(d)). As a result, a ring was formed on the surface by deposited particles around the bubble (see Fig. 2(e)). At ten hours after the heating laser being turned off, we still observed the stable accumulation pattern in the microscopy. In order to give direct evidence, the movement of particles was recorded. The results are given in Fig. 2(a–c) and Movie S2 in the ESI†. With incident laser power being 250 mW, the range of convection flow was above $500 \mu\text{m}$, which meant that the particles from a distance of above $500 \mu\text{m}$ away from the laser spot can be captured by the convective flow and carried to the bubble. In the process, the maximal moving speed of the particle reached $25 \mu\text{m s}^{-1}$.

Manipulation of the vapor bubble with the laser

As the bubble was created by the laser, we were able to change the position of the bubble through moving the focusing spot. In the above experiment, the bubble adhered to the laser spot on the

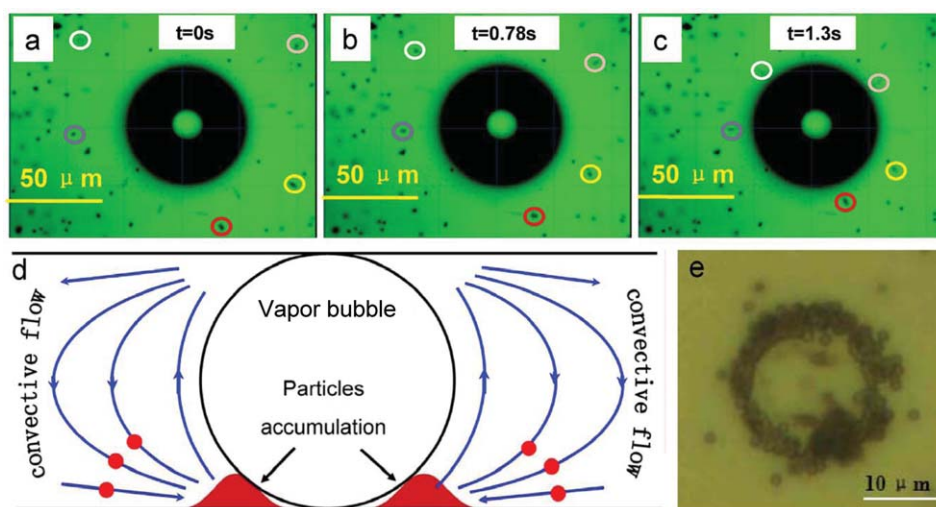


Fig. 2 (a–c) Pictures showing the movement of particles near the bubble (marked by different color circles) at different moments, which are captured by the flow and dragged to the bubble; (d) a cartoon showing the convective flow and movement of particles around the bubble; and (e) a picture showing a ring formed by accumulated particles around the bubble.

silver film, and the focused laser spot supplied energy to the bubble continually. When we changed the location of the laser spot on the film, the bubble was dragged by the laser spot and moved as a result. This is an interesting phenomenon that has not been reported previously based on our knowledge. In our following experiments, we kept the laser spot unchanged and moved the object stage of the microscope in all directions. As a result, the location of the laser spot on the film is shifted through this way. The process is described in Fig. 3(a–f) and Movie S3 in the ESI†. At the beginning, with the laser turned on, a bubble was created on the silver film, with the green laser spot located at the center of the bubble–film interface, as shown in Fig. 3(a). Then we shifted the focusing spot on the film in various directions. The direction of relative motion of the laser spot on the film is presented as white arrows in the figures. Simultaneously, the bubble was moved by the focusing spot in the process (see Fig. 3(b–e)). Because of the time delay between the laser heating and the increased localized temperature in the movement, the laser spots were not located at the center of the bubble–film interface, but at the forefront of the movement direction. In the experiment, the moving speed of a 300 μm bubble reached $300 \mu\text{m s}^{-1}$ (see ESI†, Movie S3). This is denoted as the green spot in Fig. 3(b–e). However, when the focusing spot moved exceedingly fast (above $320 \mu\text{m s}^{-1}$), the temperature of the silver film was not rapidly increased to boiling point before the laser spot left; thus, the bubble was thrown back, as shown in Fig. 3(f).

Direct-write microparticle patterns

As discussed above, the particles were first accumulated under the bubble. Then, when the bubbles were moved, the particles were deposited along the route in which the bubble passes through. Afterwards, we directly wrote any micropatterns with the accumulated particles on the silver film. The process is described in Fig. 4(a) and Movie S4 in the ESI†. Two micropatterns written by this method are given in Fig. 4(b and c).

Actually, many other complicated patterns could be possibly fabricated with this method. The statistical data show that the average linewidth of the pattern was about $26.4 \mu\text{m}$ and the

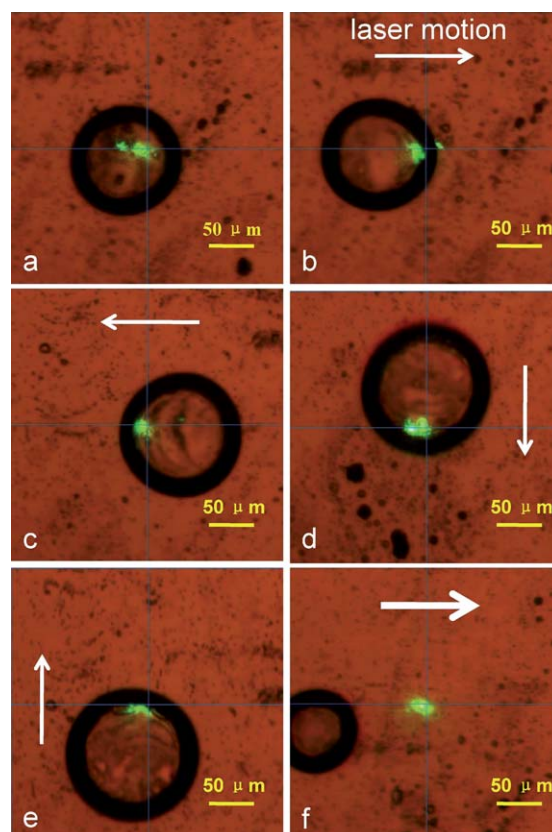


Fig. 3 Manipulating a vapor bubble by a laser spot. (a) A bubble created by laser; (b–e) pictures showing the bubble moved by the laser spot in various directions (white arrows representing the relative moving directions of the laser spot on the film); and (f) the laser spot is moving too fast and the bubble is thrown off.

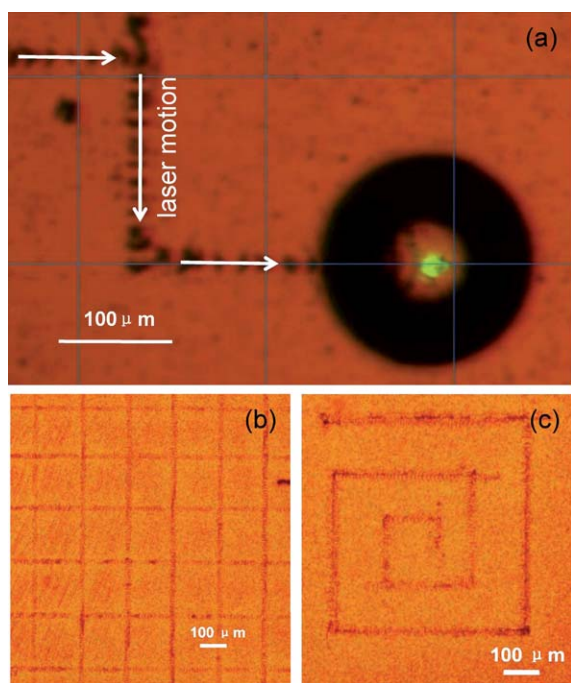


Fig. 4 (a) A picture showing the particles accumulated along the route the bubble passes through (white arrows presenting the relative moving direction of the bubble on the film); two micropatterns of particles written by the bubble: (b) square lattice and (c) Swiss roll.

standard deviation was $3.1 \mu\text{m}$. In the writing process, there are some factors that determine the minimal resolution of the write field. The first one is the size of particles. When the size of particles was too large, they were hardly driven by convection flow. Due to the van der Waals force, they fell down and adhered to the film quickly. On the other hand, if the size of particles was too small, the strong Brownian motion results in quick and random movements of particles. They were not easily accumulated by the bubble. As a result, these reduced the quality of the pattern. Appropriate particles diameter will heighten the quality of the pattern. The second one is the size of vapor bubbles: the smaller the vapor bubbles, the higher the precision. The third one is the stability of the microscope specimen stage: the higher the stability of the stage, the higher the precision. In order to give more details about our experiment, the data of some experimental parameters are provided in Table 1.

Further discussion

Compared with other accumulation techniques reported before, there are some advantages of the method proposed in this work. Firstly, in some reported experiments, a thermophoretic effect plays a crucial role in the accumulation. However, in our experiment, convection plays a more important role in the accumulation process. Generally the thermophoretic effect induced moving speed is usually slow ($0.04\text{--}0.55 \mu\text{m s}^{-1}$). In our experiment, the moving speed of particles carried by convection flow is about $25 \mu\text{m s}^{-1}$, which is much faster than the movement by the thermophoretic effect. Secondly, in our experiments, the position of accumulated particles is decided by the vapor bubble. When we move the bubble, the accumulation spot is moved correspondingly. Thirdly, water does not absorb light in the

Table 1 Data of some experimental parameters

Parameters	Values
Thickness of the water sheet	$120 \mu\text{m}$
Thickness of the Ag film	100nm
Diameter of particles	$1 \mu\text{m}$
Laser power	250mW
Laser wavelength	532nm
Laser beam waist	$106 \mu\text{m}$
The range of convection flow	$>500 \mu\text{m}$
Accumulation speed of particle	$<25 \mu\text{m s}^{-1}$
Moving speed of the bubble	$<300 \mu\text{m s}^{-1}$
Average line-width of the pattern	$26.4 \pm 3.1 \mu\text{m}$
Accumulation last time	$>10 \text{hours}$

visible region as readily as it does in the near infrared region.²³ However, the metal film can absorb the visible light and transfer the energy to water. In the present work, the efficient light absorption of the silver film enhanced the photothermal effect and played a key role in creating strong convective flow and vapor bubble. Without the silver film, the vapor bubble cannot be created even with the maximum power of our laser (400mW). Finally, the reported method in this work was simple and easy to manipulate. Only a weakly focused visible laser was needed, without any other complex experimental techniques, such as an active feedback control system, a micro-flow system, *etc.* Moreover, this simple method can be applied to accumulate various kinds of microparticles, such as silica, latex, polystyrene, and biomolecules. In this work, we only write some simple patterns with the technique in this work. It is also possible to fabricate more sophisticated patterns with higher resolution if the method is improved in the future.

Conclusion

In conclusion, we have found a simple and efficient way to directly write micropatterns with accumulated particles. Due to the enhanced photothermal effect from the silver film, a low power CW laser was used to create a vapor bubble and a thermal convection flow around it. With the help of thermal convection flow, microparticles were captured and accumulated around the bubble. Manipulating the vapor bubble allowed us to create a micropattern on the silver film formed by the accumulated microparticles. This technique has prospective applications in microfluidics, drug delivery, virus detection, and other biochip techniques. For example, fast concentration and patterning of live viruses on metal surfaces can enhance the sensitivity of their detection from biological media without damaging the virus structure.²⁴ Another example is that concentration and patterning of live cells by this technique can be used for the development of artificial architectures, live cells lithography and to create synthetic tissue. Especially, it is possible to create a synthetic colony. Assembling a synthetic structure that resembles a real-world bacterial colony could be the key to tuning the behavior of bacteria or discovering an antibiotic for inhibiting infection.²⁵

Acknowledgements

This work was supported by the National Natural Science Foundation of China (Grant Nos. 11074119, 11021403,

10874081, and 60990320), and by the National Key Projects for Basic Researches of China (Grant Nos. 2010CB630703 and 2012CB921501).

References

- 1 S. Noda and T. Baba, *Roadmap on Photonic Crystals*, Kluwer Academic Publishers, Dordrecht, Boston, 2003.
- 2 D. G. Grier, *Nature*, 2003, **424**, 810–816.
- 3 S. Tan, H. A. Lopez, C. W. Cai and Y. G. Zhang, *Nano Lett.*, 2004, **4**, 1415–1419.
- 4 P. M. Hansen, V. K. Bhatia, N. Harrit and L. Oddershede, *Nano Lett.*, 2005, **5**, 1937–1942.
- 5 M. Dienerowitz, M. Mazilu and K. Dholakia, *J. Nanophotonics*, 2008, **2**, 021875.
- 6 L. Bosanac, T. Aabo, P. M. Bendix and L. B. Oddershede, *Nano Lett.*, 2008, **8**, 1486–1491.
- 7 A. H. J. Yang, S. D. Moore, B. S. Schmidt, M. Klug, M. Lipson and E. David, *Nature*, 2009, **457**, 71–75.
- 8 H. X. Xu and M. Käll, *Phys. Rev. Lett.*, 2002, **89**, 246802.
- 9 G. Volpe, R. Quidant, G. Badenes and D. Petrov, *Phys. Rev. Lett.*, 2006, **96**, 238101.
- 10 M. Righini, A. S. Zelenina, C. Girard and R. Quidant, *Nat. Phys.*, 2007, **3**, 477–480.
- 11 A. N. Grigorenko, N. W. Roberts, M. R. Dickinson and Y. Zhang, *Nat. Photonics*, 2008, **2**, 365–370.
- 12 M. Righini, P. Ghenuche, S. Cherukulappurath, V. Myroshnychenko, F. J. Gabajo and R. Quidant, *Nano Lett.*, 2009, **8**, 3387–3391.
- 13 K. Wang, E. Schonbrun, P. Steinvurzel and K. B. Crozier, *Nano Lett.*, 2010, **10**(9), 3506–3511.
- 14 W. H. Zhang, L. N. Huang, C. Santschi and O. J. F. Martin, *Nano Lett.*, 2010, **10**, 1006–1011.
- 15 E. David, S. Xavier, Y. F. Chenac and M. Sudeep, *Lab Chip*, 2011, **11**, 995–1009.
- 16 R. D. Leonardo, F. Ianni and G. Ruocco, *Langmuir*, 2009, **25**(8), 4247–4250.
- 17 S. J. Williams, A. Kumar, N. G. Green and S. T. Wereley, *Nanoscale*, 2009, **1**, 133–137.
- 18 D. Braun and A. Libchaber, *Phys. Rev. Lett.*, 2002, **89**, 188103.
- 19 V. G. Chávez, R. Quidant, P. J. Reece, G. Badenes, L. Torner and K. Dholakia, *Phys. Rev. B: Condens. Matter Mater. Phys.*, 2006, **73**, 085417.
- 20 S. Dühr and D. Braun, *Phys. Rev. Lett.*, 2006, **97**, 038103.
- 21 C. B. Mast and D. Braun, *Phys. Rev. Lett.*, 2010, **104**, 188102.
- 22 K. Zhang, A. Q. Jian, X. M. Zhang, Y. Wang, Z. H. Lib and H. Y. Tam, *Lab Chip*, 2011, **11**, 1389–1395.
- 23 M. J. Weber, *Handbook of Optical Materials*, CRC Press, Boca Raton, 2003.
- 24 A. A. Yanik, M. Huang, O. Kamohara, A. Artar, T. W. Geisbert, J. H. Connor and H. Altug, *Nano Lett.*, 2010, **10**(12), 4962–4969.
- 25 M. Mir, P. Matsudaira and G. Timp, *Lab Chip*, 2008, **8**, 2174–2181.